

Active mixing of immobilized enzymatic system in microfluidic chip

K.A. Lukyanenko¹, K.I. Belousov³, I.A. Denisov¹, A.S. Yakimov¹, E.N. Esimbekova^{1,2}, A.S. Bukatin¹, A.A. Evstrapov⁴ and P.I. Belobrov^{1,2}

¹ Siberian Federal University, Krasnoyarsk 660041, Russia

² Institute of Biophysics SB RAS, Krasnoyarsk 660036, Russia

³ ITMO University, Saint Petersburg 197101, Russia

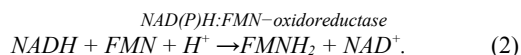
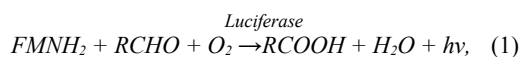
⁴ Institute for Analytical Instrumentation, Saint Petersburg 198095, Russia

E-mail: kirill.lukyanenko@gmail.com

Parameters for sample loading, dried reagents dissolution and mixing with sample for bienzyme system NAD(H):FMN-oxidoreductase and luciferase immobilized in microfluidic chip were successfully determined. Numerical simulations of reaction chamber geometry, FMN escape from starch gel and mixing options were conducted to achieve higher sensitivity of bioluminescent reaction. Results of numerical simulations were verified experimentally. The active mixer for dried reagents was made from an electro-mechanical speaker's membrane which was connected to the input of the chip. Such a mixer provided better efficiency than a passive mixing, and it is simple enough for use in point-of-care devices with any systems based on immobilized enzymes in chips

1. Introduction: One of the upcoming trends in analytical instrumentation is switching routine analytical assays into miniaturized and automated point-of-care (POC) devices [1, 2]. Essential components of such devices are disposable chips which are inexpensive and easy to fabricate [3, 4]. These smart biochips accommodate all the assay components viz. sample preparation chamber, reagents mixing platform and provision for simultaneous signal detection with minimum periphery equipments. Disposable chips have huge potential in many fields of medicine and ecology through their customization.

In the present research, we describe disposable microfluidic chip for environmental monitoring using bacterial luciferase based bioassay. The biological module described herein is based on bienzyme bioluminescent system [5]. The interaction of contaminants in water samples with enzymes of bioluminescent bacteria leads to parametric changes in bioluminescent system catalyzed by NAD(P)H:FMN-oxidoreductase and luciferase [6]:



These changes are expressed in the reduction of maximum light emission intensity as compared with the control sample. Thus it is possible to obtain an integral assessment of the analyte toxicity.

The biological module was immobilized in a suitable matrix and subsequently dried and sealed in the designed microfluidic chip. The immobilized components of the reaction chamber (Fig.1) must mix uniformly while receiving the aqueous sample (environmental contaminants) to respond precisely. These pre-requisites required special arrangements to promote efficient mixing process since reagents (i) needed to exit from the gel followed by (ii) their uniform distribution across the reaction chamber to avoid erroneous results.

The requirement for compactness and placement of all analytical steps into a single chip makes the reagent mixing process complicated due to low Reynolds numbers [7]. Today there are many passive and active mixers available for different types of chemical reactions [8]. Most of the commercially successful POC devices use passive mixing [9].

However, different passive mixers are based on curved microchannels and colliding substreams [10] which are not effective

enough when dealing with dried reagents. Among many types of active mixers [8], only acoustic mixers have the potential to provide necessary mixing efficiency without affecting enzyme activity.

The aim of the current research was to determine the parameters of sample loading, efficient dissolution of dried reagents and their subsequent uniform mixing with assay sample in the microfluidic chip for performing enzymatic bioassays applicable in environmental monitoring.

Formation of air bubble during the introduction of sample is a key factor that contributes to the subsequent qualitative mixing. The lower the rate of sample entry, the less is the likelihood of bubbles formation. At the same time, the sample introduction rate must be high enough to avoid any premature dissolution and passive mixing of immobilized substrates of bioluminescent reaction. To achieve this goal it was necessary (i) to determine the optimal shape of the reaction chamber and flow velocity for sample entry using numerical simulation.

Due to the passive drying of FMN in a starch gel its total amount participating in the reaction will depend on the characteristics of FMN escape from the gel. It is necessary (ii) to create an adequate model of FMN escape to predict this amount and determine the suitable time for reagents dissolution.

Enhanced signal response and reproducibility of bioluminescent reaction required uniform distribution of FMN concentration in reaction chamber during analysis for which time resolved spectroscopy method could be used since FMN has a color. Deciphering the optimum mixing algorithm required (iii) selection of the amplitude and frequency of liquid oscillations in the chip, which would provide the lowest coefficient of variation of FMN concentration throughout the reaction chamber.

2. Experimental:

2.1. Microfluidic chips: Body of the chip was fabricated using industrial quality poly(methyl methacrylate) (PMMA) by micromilling method with CNC milling machine Modela MDX-20 (Roland, Japan). The depth of the channels was 0.5 mm. The chips were sealed at room temperature using 1,2-dichloroethane and controlled pressure. The design of chip with biological components is shown in Fig.1.

2.2. Biological module: Biological module inhabit two dried starch gel droplets. The first 10 μ l droplet contained coupled enzymatic system: bacterial luciferase (*Photobacterium leiognathi*) and

NAD(P)H:FMN-oxidoreductase (*Vibrio fischeri*) in addition to reduced nicotinamide adenine dinucleotide (NADH) and tetradecanal. The second 5 μ l droplet contained flavin mononucleotide (FMN) to initiate the bioluminescence reaction. Both droplets were dried on a gelatin scaffold on the surface of the reaction chamber.

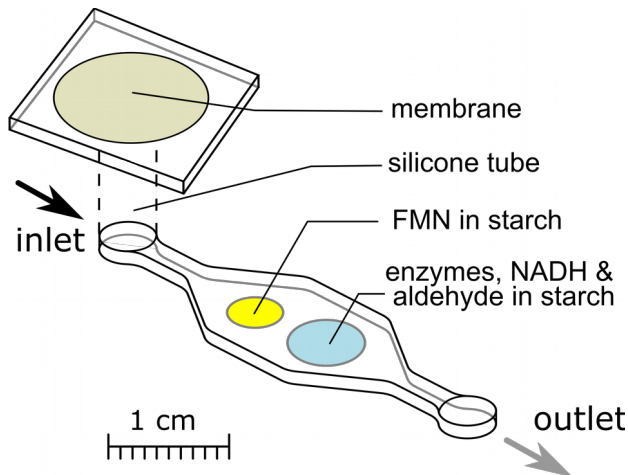


Fig. 1 Schematic representation of the microfluidic chip with connected mixer.

2.3. Numerical simulations: Calculations of flow movement and the diffusion of FMN in microchannels was conducted with COMSOL Multiphysics (COMSOL, Sweden) using finite element method. The system of Navier-Stokes equations was used for simulation of liquid velocity profile. The displacement of the border between two phases during chip filling was calculated by level set method. The calculation of convective and diffusive transport was performed with Fick's second law with the added convective term. The quality of mixing was determined by calculating coefficient of variation. For simulation 2d-axisymmetric and 2D models were used.

2.4. Concentration measurement: Uniform distribution of reagents in the reaction chamber of the microfluidic chip was assessed through time-resolved spectroscopy by HSV palette analysis. For this AxioCam ICc 5 and Axio Scope A1 microscope (Carl Zeiss, Germany) were used. Image of the reaction chamber was acquired with the camera and then saturation level of HSV palette was analyzed with proprietary software. The software was written with BlackBox Component Builder (Oberon microsystems Inc, Switzerland).

2.5. Mixing: The active mixer was made from a speaker's electromechanical membrane which was connected to the input of the inlet channel of the chip. The membrane was 14 mm in diameter and the resistance was 33 Ohm. The signal pattern for membrane movement was generated by a laboratory self-made device. It consisted of the LPC2103 MCU (NXP, Netherlands), several optrons and transistors which controlled the H bridge allowing voltage to be applied across the membrane in either direction. Signals were programmed and sent to this amplifier using the software made with BlackBox Component Builder (Oberon microsystems Inc, Switzerland). Membrane oscillations with predefined patterns created acoustic wave, which led fluid movement in the chip.

3. Results and discussion:

3.1. Reaction chamber design: While filling the chip's reaction chamber with liquid during sample introduction, there is a risk of air bubbles formation. These bubbles can affect the bioluminescent reaction by increasing measurement error. One way to solve this problem is to increase the hydrophilicity of the channels. However, channel treatment using UV radiation [11, 12], plasma [13, 14] or other methods may damage the biological materials.

Due to immobilization of biological components in form of two droplets of dried gel, the diamond shape of the reaction chamber was chosen as basic design. One can minimize the formation of bubbles by optimizing the geometry of the diamond-shaped reaction chamber, namely the expansion angle ϕ under which it widens. Through optimization, we considered the threshold fluid flow velocity in the reaction chamber that starts bubble formation. At optimal flow speed, the probability of bubble formation was minimized.

Numerical simulation was performed for filling the empty reaction chamber with water taking various expansion angles into consideration. All variants ranged with ϕ : from 110° to 170° . With every geometry, the reaction chamber remained relatively compact, not greater than 15 mm in length and 6 mm in width. The square area remained approximately equal to 40 cm^2 in all cases. Reaction chamber was initially filled with air.

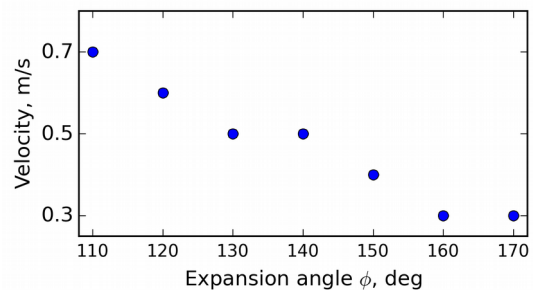


Fig. 2 Minimum velocity for different expansion angles ϕ when bubble formation begins.

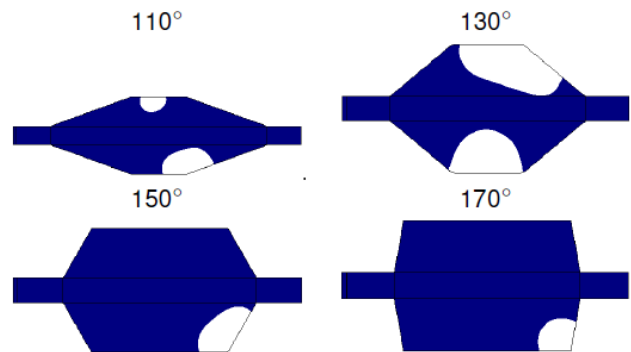


Fig. 3 Examples of bubbles (white) that formed during the filling of the reaction chamber with water (blue) during simulation.

The water filled the reaction chamber at constant velocity. Boundary condition for walls was wetted wall. Wetting angle for PMMA used in this work was $70 \pm 5^\circ$.

The minimum flow velocity at which bubble formation begins at different ϕ angles was studied. As shown in Fig. 2, the results of the numerical simulation indicate that minimum flow velocity at which bubble formation begins gradually reduces from 0.7 m/s for 110° to 0.3 m/s at 170° . Examples of main types of bubbles are shown in Fig. 3.

Based on these results, in further experiments, we used 120° expansion angle (Fig. 1) in the reaction chamber. This angle was chosen due to the optimum dimensions of the reaction chamber and high flow threshold velocity of 0.6 m/s at which the bubble formation may begin. This high velocity ensures the lowest probability of bubble formation during sample introduction.

3.2. FMN escape from the starch gel: The processes involving FMN and enzymatic escape from the starch gel have significant influence on the quality of mixing. It is necessary to determine the time at which most of the FMN escapes the starch gel to achieve uniform FMN distribution in the reaction chamber after mixing.

Simulation results were compared with experimental data of FMN diffusion (Fig. 4) that were acquired using time-resolved spectroscopy method. Experimental rates of concentration change dc/dt were obtained with an average interval of 0.4 seconds. The data was noisy due to the small size of the gel droplet (5 μ l) and the error of the measurement. Nevertheless, successful smoothing was performed using FFT filter with cutoff frequency equal to 0.08 (Fig. 5, green line). In Fig. 5 and Fig. 6 the presented concentration value per unit area relates to two-dimensional nature of experimental images. It should be noted that the parameter of FMN distribution in gel and the dynamics of gel swelling remain unknown.

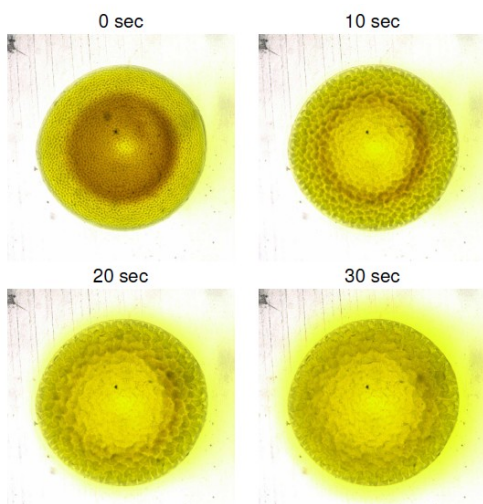


Fig. 4 FMN diffusion from the starch droplet in the microfluidic chip after water sample injection.

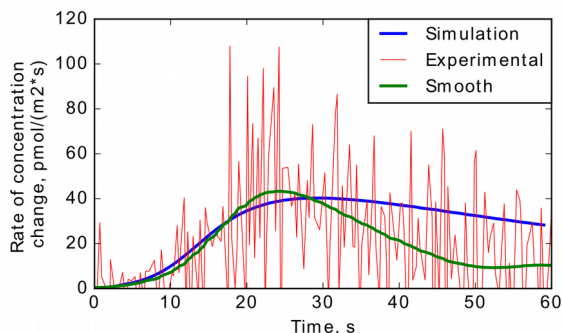


Fig. 5 The rate of concentration change dc/dt of numerical simulation and experimental data 80 μ l from the gel boundary. Blue - simulation, red - experimental data, green - smoothed data.

The process of FMN escape involves two steps: dissolution of FMN crystals in liquid and diffusion of FMN from the gel. The simulation

showed that dissolution led to a continuous decrease of the escape velocity while the experiment on the contrary indicated the increase of escape velocity at the beginning. So the diffusion spread has a priority. In the following simulation only diffusion was considered.

The fitting of the simulation results was carried out based on the value of the rate of concentration change at a distance of 80 μ m from the border of the gel as shown in Fig. 5. The distance of 80 μ m was selected as sufficiently close to the border of the gel to reflect changes in the concentration at the initial stage of the experiment. At the same time it was sufficiently remote that the results were not influenced by the effects associated with the transition between gel and solution. The steep decline in concentration change after 25 second shown in Fig. 5 relates to the out of range and simulation data should have slower decrease.

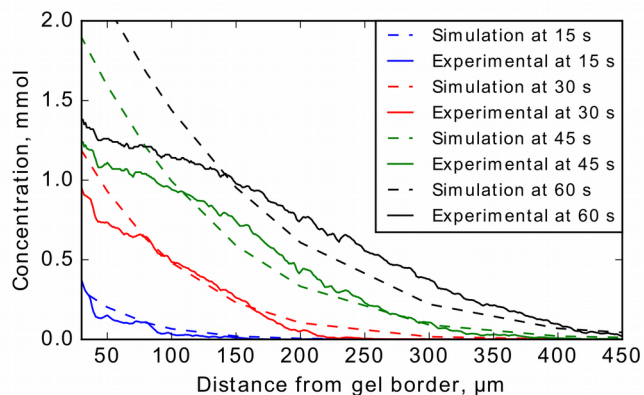


Fig. 6 Concentration distribution profile at various times. Solid lines – experimental data, dotted lines – simulation data.

Such dependence can be achieved using the initial concentration distribution of FMN in gel with linear decrease to 0 from the radius center to the gel border and the following diffusion coefficient D_{gel} :

$$D_{gel} = \frac{D_{gel}^{max}}{1 + \exp\left(-\frac{t-T_1}{T_2}\right)}, \quad (3)$$

where $T_1 = 10$ s – the position of the inflection point, $T_2 = 2.5$ s – time constant, $D_{gel}^{max} = 0.75 D_{sol}$ – value of the diffusion coefficient at the end of the swelling [15], $D_{sol} = 4.8 \cdot 10^{-10}$ m²/s – diffusion coefficient of FMN in the liquid [16]. As a result, the coincidence of concentrations throughout the experiment was achieved (Fig. 6).

Based on this model, the time for beginning of mixing after sample introduction was chosen at 30th second when most of the FMN escapes the gel.

3.3. Active mixing parameters simulations: The intensity of bioluminescence and the measurement error is largely dependent on the uniform distribution of FMN concentration in the reaction chamber after its escape from the gel. This uniformity can be mathematically expressed using the coefficient of variation (CV) for FMN concentration in the reaction chamber. Lower level of CV reflects more uniform distribution of FMN concentration. Sinusoidal and square liquid flow oscillations with 3 and 4 μ l amplitude at constant and variable frequencies were used to improve mixing.

2D numerical simulations were performed to investigate the distribution of FMN in the reaction chamber after the mixing at different frequencies. The basic procedure of FMN concentration

simulation in a microfluidic chip was demonstrated previously [17]. Results of the mixing simulations at 1-10 Hz frequency are shown in Fig. 7. FMN was initially located in the left half of the reaction chamber. When mixing started, the first push at low 1 Hz frequency moved FMN in the area of immobilized bioluminescent components. Every next push was in the opposite direction according to the signal pattern shown in Fig. 8. Subsequent growth of the oscillation frequency provided uniform distribution of FMN concentration throughout the reaction chamber by the 3rd second.

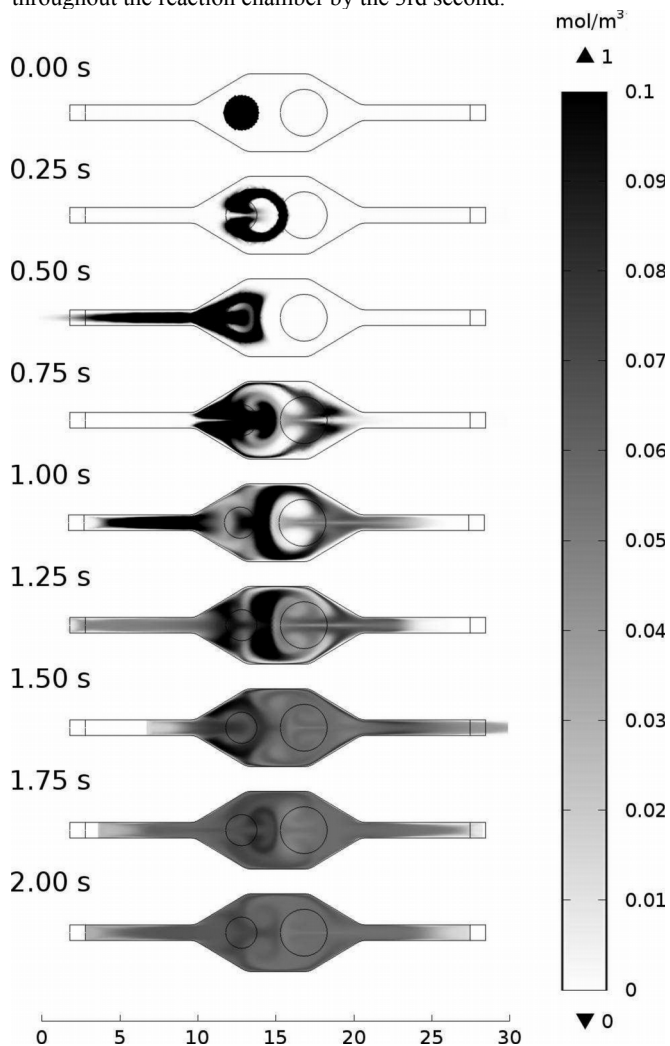


Fig. 7 Simulation of FMN mixing in chip at 1-10Hz oscillation frequency.

It was observed that, at frequencies over 10 Hz, the form of the liquid streams in the chamber changed, resulting in reduced mixing efficiency per cycle. Rectangular flow oscillation with a constant frequency showed the least efficient mixing, however, the use of variable frequency provided the same value as the sinusoidal signal as shown in Fig. 9. Thus, the variable frequency of signal can increase the mixing efficiency in one period of oscillation, since at the same value of the CV, it has an average frequency of 5 Hz. Increase of oscillation amplitude up to 4 μ l using this mode allowed to achieve CV value of FMN concentration in the reaction chamber equal to 0.01 by the 3rd second.

We used mixing parameters with gradual increase of oscillation frequency from 1 to 10 Hz for 3 seconds as shown in Fig. 8 due to the lowest CV of FMN for the experiments.

3.4. Bioluminescence intensity measurements: Results of numerical simulation for chosen reaction chamber geometry, mixing parameters and FMN gel escape observation were verified experimentally. Time-resolved spectroscopy by HSV palette analysis was used for this purpose.

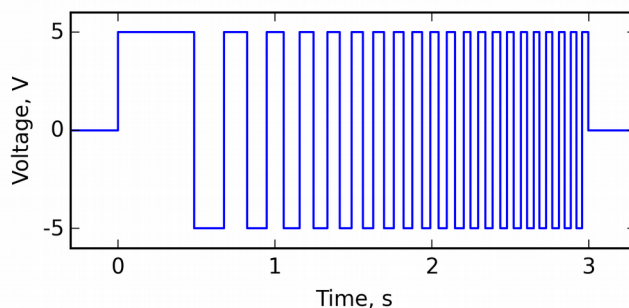


Fig. 8 Mixing pattern for 1-10Hz frequency.

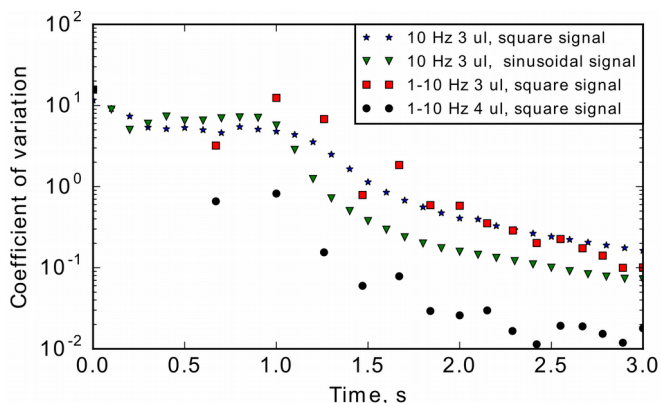


Fig. 9 Coefficient of variation of FMN distribution in the area of enzymes location (Fig. 1) in the reaction chamber of microfluidic chip at the two-dimensional simulation with different signal forms and fluid oscillation amplitude.

Experimental verification showed that the intensity of the luminescence signal at the selected mixing parameters increased by several times (Fig. 10, A, solid line) from 2000 to 12000 RLU when applying active mixing compared to passive mixing (Fig. 10, A, dotted line). After the beginning of mixing at the 10th second, the FMN concentration distribution became uniform all around the reaction chamber (Fig. 10, B) and increased from 0.02 to 1.2 mM. Application of active mixing provided the most uniform distribution of FMN concentration in the reaction chamber of the chip and thus reduced the standard deviation to a level of 25% compared to passive mixing. Further studies showed similar results at constant rectangular frequency of 8 Hz.

The efficiency of the selected mode of mixing may be explained as follows. The velocity profile has a parabolic shape at lower frequencies of fluid oscillation, whereby, FMN at the initial cycles is more evenly distributed throughout the area of the reaction chamber (Fig. 10, B). Subsequent lift of frequency and intensity of pulses resulted in eventual most efficient mixing.

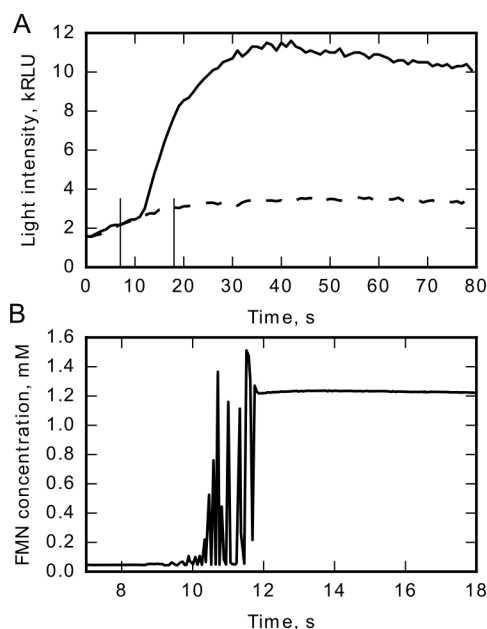


Fig. 10 A) Luminescence kinetics without active mixing (dotted line) and with active mixing (solid line) in microfluidic chip. Two vertical lines indicate the time interval that was used for figure below; B) FMN concentration in the area of immobilized bioluminescent components when mixing starts at the 10th second of luminescence measurement.

4. Conclusions: The selected design of the reaction chamber allowed the most efficient use of limited space on a chip and provided the lowest probability of bubble formation during sample introduction.

Numerical simulation and experimental observation of FMN escape from the gel allowed to predict its concentration at different times to find the proper time when mixing began.

The use of the variable frequency of liquid oscillations allowed achieving the lowest coefficient of variation of FMN concentration in the reaction chamber.

Results of the numerical simulations were verified experimentally. The selected mixing parameters enabled to provide reagents escape from the dried gel and to achieve a uniform distribution of FMN in the reaction chamber which led to achieve higher bioluminescent signal maintaining assay reproducibility. The mixing did not affect the kinetics of bioluminescence because the duration of mixing (3 s) was less than the time required to reach the maximum intensity of luminescence.

The proposed approach for dried reagents mixing may be used with many other microfluidic systems in fabricating point-of-care devices.

5. Acknowledgment: The research was supported by the grant of the Russian Science Foundation (project no.15-19-10041).

6 References

- [1] Gubala V., Harris L.F., Ricco A.J., *et al.*: 'Point of care diagnostics: Status and future', *Analytical Chemistry*, 2012, 84, (2), pp. 487–515
- [2] Jung W., Han J., Choi J., Ahn C.H.: 'Point-of-care testing (POCT) diagnostic systems using microfluidic lab-on-a-chip technologies', *Microelectronic Engineering*, 2015, 132, pp. 46–57
- [3] Mark D., Haerberle S., Roth G., *et al.*: 'Microfluidic lab-on-a-chip platforms: requirements, characteristics and applications', *Chemical Society Reviews*, 2010, 39, (3), pp. 1153–1182

- [4] Evstrapov A.A.: 'Microfluidic chips for biological and medical research', *Russian Journal of General Chemistry*, 2012, 82, (12), pp. 2132–2145
- [5] Roda A., Mirasoli M., Michelini E., *et al.*: 'Progress in chemical luminescence-based biosensors: A critical review', *Biosensors and Bioelectronics*, 2016, 76, pp. 164–179
- [6] Kratasyuk V.A., Esimbekova E.N.: 'Applications of luminous bacteria enzymes in toxicology', *Combinatorial chemistry and high throughput screening*, 2015, 18, (10), pp. 952–959
- [7] Weigl B., Domingo G., LaBarre P., Gerlach J.: 'Towards nonand minimally instrumented, microfluidics-based diagnostic devices', *Lab on a Chip*, 2008, 8, (12), pp. 1999–2014
- [8] Lee C.Y., Chang C.L., Wang Y.N., Fu L.M.: 'Microfluidic mixing: a review', *International journal of molecular sciences*, 2011, 12, (5), pp. 3263–3287
- [9] Chin C.D., Linder V., Sia S.K.: 'Commercialization of microfluidic point-of-care diagnostic devices', *Lab on a Chip*, 2012, 12, (12), pp. 2118–2134
- [10] Gervais L., De Rooij N., Delamar E.: 'Microfluidic chips for point-of-care immunodiagnosics', *Advanced Materials*, 2011, 23, (24)
- [11] Wei S., Vaidya B., Patel A.B., *et al.*: 'Photochemically patterned poly(methyl methacrylate) surfaces used in the fabrication of microanalytical devices.', *The journal of physical chemistry. B*, 2005, 109, (35), pp. 16988–16996
- [12] Shah J.J., Geist J., Locascio L.E., *et al.*: 'Surface modification of poly(methyl methacrylate) for improved adsorption of wall coating polymers for microchip electrophoresis', *Electrophoresis*, 2006, 27, (19), pp. 3788–3796
- [13] Long T.M., Prakash S., Shannon M.a., Moore J.S.: 'Watervapor plasma-based surface activation for trichlorosilane modification of PMMA.', *Langmuir : the ACS journal of surfaces and colloids*, 2006, 22, (9), pp. 4104–4109
- [14] Vesel A., Mozetic M.: 'Surface modification and ageing of PMMA polymer by oxygen plasma treatment', *Vacuum*, 2012, 86, (6), pp. 634–637
- [15] Muhr A., Blanshard J.: 'Diffusion in gels', *Polymer*, 1982, 23, (7), pp. 1012–1026
- [16] Nguyen H.D., Renslow R., Babauta J., *et al.*: 'A voltammetric flavin microelectrode for use in biofilms', *Sensors and Actuators B: Chemical*, 2012, 161, (1), pp. 929–937
- [17] Belousov K.I., Denisov I.A., Lukyanenko K.A., *et al.*: 'Dissolution and mixing of flavin mononucleotide in microfluidic chips for bioassay', *Journal of Physics: Conference Series*, 2016, 741, (1), pp. 012058